AIP | Biomicrofluidics
Fundamentals, Perspectives & Applications

An unexpected particle oscillation for electrophoresis in viscoelastic fluids through a microchannel constrictiona)

Xinyu Lu, Saurin Patel, Meng Zhang, Sang Woo Joo, Shizhi Qian, Amod Ogale, and Xiangchun Xuan

Citation: Biomicrofluidics **8**, 021802 (2014); doi: 10.1063/1.4866853
View online: http://dx.doi.org/10.1063/1.4866853
View Table of Contents: http://scitation.aip.org/content/aip/journal/bmf/8/2?ver=pdfcov
Published by the AIP Publishing

An unexpected particle oscillation for electrophoresis in viscoelastic fluids through a microchannel constriction[a)]

Xinyu Lu,[1] Saurin Patel,[1] Meng Zhang,[2] Sang Woo Joo,[3,b)] Shizhi Qian,[4] Amod Ogale,[2] and Xiangchun Xuan[1,b)]
[1]*Department of Mechanical Engineering, Clemson University, Clemson, South Carolina 29634-0921, USA*
[2]*Department of Chemical and Biomolecular Engineering, and Center for Advanced Engineering Fibers and Films, Clemson University, Clemson, South Carolina 29634-0909, USA*
[3]*School of Mechanical Engineering, Yeungnam University, Gyongsan 712-719, South Korea*
[4]*Institute of Micro/Nanotechnology, Old Dominion University, Norfolk, Virginia 23529, USA*

(Received 26 November 2013; accepted 17 January 2014; published online 3 March 2014)

Electrophoresis plays an important role in many applications, which, however, has so far been extensively studied in Newtonian fluids only. This work presents the first experimental investigation of particle electrophoresis in viscoelastic polyethylene oxide (PEO) solutions through a microchannel constriction under pure DC electric fields. An oscillatory particle motion is observed in the constriction region, which is distinctly different from the particle behavior in a polymer-free Newtonian fluid. This stream-wise particle oscillation continues until a sufficient number of particles form a chain to pass through the constriction completely. It is speculated that such an unexpected particle oscillating phenomenon is a consequence of the competition between electrokinetic force and viscoelastic force induced in the constriction. The electric field magnitude, particle size, and PEO concentration are all found to positively affect this viscoelasticity-related particle oscillation due to their respective influences on the two forces. © *2014 AIP Publishing LLC*.
[http://dx.doi.org/10.1063/1.4866853]

I. INTRODUCTION

Electrophoresis plays an important role in many applications such as capillary electrophoresis and electrokinetic micro/nanofluidics, etc.[1] It is the motion of a charged particle with respect to a suspending fluid under the application of an electric field. The fluid can be either infinite for which particle electrophoresis resembles particle sedimentation in a stationary fluid or confined in a channel where particle electrophoresis is almost always accompanied by fluid electroosmosis.[2] While particle electrophoresis in both cases has been extensively investigated in the past, the majority of these studies concern only Newtonian fluids.[3] Due to the shear-rate-independent viscosity of these fluids, electrophoresis and electroosmosis are both a linear function of the applied electric field and the surface charge (or zeta potential) of the particle/channel.[4] However, many of the fluids used in capillary electrophoresis and microfluidic devices are polymer solutions[5–8] and biofluids[9–12] which are complex. They often possess a shear-rate-dependent viscosity and may even exhibit elastic or plastic effects.[13–16] Consequently, electrophoresis in and electroosmosis of these non-Newtonian fluids could be significantly different from those with Newtonian fluids.[17–19]

A number of theoretical (including numerical) studies have been recently reported on electroosmosis of non-Newtonian fluids whose rheology is characterized by various constitutive

[a)]Paper submitted as part of a special collection covering contributions related to the American Electrophoresis Society's symposium at the SciX 2013 meeting (Guest Editors: A. Ros, E. D. Goluch) held in Milwaukee, Wisconsin, September 29–October 4, 2013.
[b)]Authors to whom correspondence should be addressed. Electronic addresses: xcxuan@clemson.edu and swjoo@yu.ac.kr.

equations, including the power-law,[20–30] Phan-Thien-Tanner (PTT),[31–36] Carreau,[37–39] Oldroyd-B (including Upper-Convected Maxwell, UCM[34])[40] models and others.[41–43] Nonlinear relations are obtained for the electroosmotic velocity as a function of the electric field and zeta potential. Also, the electrophoretic motion of particles in non-Newtonian fluids has been numerically predicted by Hsu and co-workers with a Carreau model.[44–51] The fluid shear-thinning effect is found to increase the particle mobility significantly as compared to that in a Newtonian fluid. Recently, Khair *et al.*[52] presented a theoretical scheme to calculate the electrophoretic motion of particles of any shape in fluids with a shear-rate-dependent viscosity. They demonstrated a shape and size dependence of particle electrophoresis due to the non-Newtonian rheology, which is markedly different from that in Newtonian fluids.[53]

To date, however, very little experimental work has been done on electroosmosis of and electrophoresis in non-Newtonian fluids. Chang and Tsao[54] observed a significant drag reduction in electroosmotic flow of polymer solutions, which increases with the ratio of the polymer size to the electric double layer thickness. Bryce and Freeman[55] demonstrated that the flow velocity of standard electroosmotic pumping is sufficient to excite extensional instabilities in dilute polymer solutions through a 2:1 microchannel constriction. Interestingly, they found later that these instabilities actually reduce the fluid mixing relative to that in polymer-free fluids.[56] Inspired by the work from Bryce and Freeman,[55,56] we conducted an experimental study of particle electrophoresis in viscoelastic polymer solutions through a microchannel constriction. An unexpected particle oscillation was observed, which was found to vary with the applied electric field, particle size, and polymer concentration. This article presents these experimental results along with our attempted explanation of the particle oscillating phenomenon.

II. EXPERIMENT

A. Preparation of non-Newtonian fluids and particle suspensions

Non-Newtonian fluids were prepared by dissolving Poly(ethylene oxide) (PEO) powder (average molecular weight is 4×10^6 Da, Sigma-Aldrich USA) into 1 mM phosphate buffer. Four concentrations of PEO were used in our experiment, 50 ppm (i.e., dissolving 50 mg of PEO powder into 1 litre of buffer), 100 ppm, 200 ppm, 500 ppm, which are all lower than its overlap concentration, $c^* = 547$ ppm, as calculated from the expression of Graessley.[57] The last quantity was obtained from $c^* = 0.77/[\eta]$, where $[\eta] = 0.072 M_w{}^{0.65}$ is the intrinsic viscosity given by the Mark-Houwink relation with $M_w = 4 \times 10^6$ g/mol being the molecular weight of PEO.[80] The shear viscosities of the four prepared PEO solutions (with no particles or surfactants being added) were measured in a Couette geometry by a rheometer (ARES LS/M, TA instruments) and found to be 1.1 mPa·s, 1.2 mPa·s, 1.4 mPa·s and 2.0 mPa·s, respectively, with a negligible variation over the range of shear rate from $50\,s^{-1}$ to $1000\,s^{-1}$. Therefore, each of these PEO solutions can be viewed as a Boger fluid,[58] which has viscoelasticity but negligible shear-thinning/thickening effects. This treatment is consistent with that in the recent work from Rodd *et al.*[59] The relaxation time of the PEO polymer was calculated to be $\lambda_Z = 1.07$ ms according to Zimm theory.[60] The effective relaxation time[61] of the PEO solutions was estimated using $\lambda_{eff} = 18\lambda_Z\,(c/c^*)$, which gives 4.07 ms, 6.39 ms, 10.01 ms, and 18.17 ms, for the prepared four concentrations. The pure buffer with no addition of the PEO polymer was used as the Newtonian fluid in our experiments for comparison. A summary of these solution properties is given in Table I.

The particle suspensions were prepared by re-suspending polystyrene spheres of 3 μm, 5 μm, and 10 μm in diameter (Sigma-Aldrich USA), respectively, into the PEO solution(s) at a final concentration of 10^6–10^7 particles per milliliter. A small amount of Tween 20 (0.5% in volume ratio, Fisher Scientific) was added to the suspensions for the purpose of suppressing the particle adhesions to microchannel walls and other particles. For comparison, 10 μm particles were also re-suspended in the pure buffer with Tween 20 being added. Polystyrene particles have a density of $1.05\,g/cm^3$, which is slightly larger than that of the suspending media. They are non-conducting in bulk, but exhibit surface conductance due to the spontaneous occurrence of electric double layer.[1,2] Their "effective" electric conductivity was estimated to be much smaller than that of the PEO solution (about 200 μS/cm) for all sizes of particles used in our

TABLE I. Solution properties.

		PEO in pure buffer (concentration c)			
Fluid property (at 20 °C)	Pure buffer	50 ppm	100 ppm	200 ppm	500 ppm
Density (g/cm^3)	0.998	0.998	0.998	0.998	0.998
Zero-shear viscosity (mPa·s)	1.0	1.1	1.2	1.4	2.0
Overlap concentration c^* (ppm)		547	547	547	547
Concentration ratio c/c^*		0.091	0.183	0.366	0.914
Zimm relaxation time, λ_Z (ms)		1.07	1.07	1.07	1.07
Effective relaxation time, λ_{eff} (ms)		4.07	6.39	10.01	18.17

experiments. Hence, they all experience negative dielectrophoresis under the gradients of DC electric fields.[3,4]

B. Microchannel fabrication

The microchannel was fabricated by the standard soft lithography technique using liquid polydimethylsiloxane (PDMS). Briefly, a negative photo mask was made by printing the channel layout, which was drawn in AutoCAD®, onto a transparent thin film at a resolution of 10 000 dpi (CAD/Art Services). A 40-μm thick SU-8-25 photoresist (MicroChem) was coated onto a clean glass slide using a spin coater (WS-400B-6npp/lite, Laurell Technologies), which started at 500 rpm for 10 s and ramped by 300 rpm/s to the terminal spin speed of 1000 rpm with a dwelling of 20 s. After a two-step soft bake (65 °C for 4 min and 95 °C for 8 min) in a hot plate (HP30A, Torrey Pines Scientific), the photoresist film was exposed through the photo mask to a 365 nm UV light (ABM Inc., San Jose, CA) for 30 s. It then underwent a two-step hard bake (65 °C for 2 min and 95 °C for 4 min) before being submerged into a SU-8 developer solution (MicroChem) for 10 min. Following a brief rinse with isopropyl alcohol (Fisher Scientific) and another two-step hard bake (65 °C for 1 min and 95 °C for 5 min), a positive replica of photoresist was left on the glass slide, which served as the mold of the microchannel (i.e., the so-called master) for reuses.

The microchannel mold was placed in a Petri dish and then covered by liquid PDMS, a mixture of Sylgard 184 and the curing agent at a 10:1 ratio in weight. After degassing in a vacuum oven (13-262-280 A, Fisher Scientific) for 15 min, the Petri dish was placed into a gravity convection oven (13-246-506GA, Fisher Scientific) at 70 °C for 3–4 h. The cured PDMS that enclosed the entire microchannel was cut using a scalpel and peeled off from the master. Two through holes of 5 mm in diameter each were made as reservoirs in the pre-defined circles at microchannel ends using a metal punch. Immediately following a plasma treating for 1 min (PDC-32G, Harrick Scientific), the channel side of the PDMS slab was irreversibly bonded to a clean glass slide. A drop of the working solution (with no particles suspended) was loaded into one of the reservoirs, which was found to fill the entire microchannel automatically by capillary force and used to maintain the channel walls hydrophilic. A picture of the fabricated PDMS/glass microchannel is shown in Fig. 1. It is 400 μm wide and 1 cm long with a uniform depth of 40 μm. It has a 40 μm wide constriction in the middle with a length of 200 μm.

C. Experimental technique

The electrokinetic motion of particles in the microchannel was induced by applying a DC electric field across the channel, which was supplied by a function generator (33220A, Agilent Technologies) in conjunction with a high-voltage amplifier (609E-6, Trek). The electric field was kept no more than 500 V/cm in order to minimize Joule heating effects.[62,63] The pressure-driven motion of particles was eliminated by balancing the liquid heights in the end reservoirs prior to each test. Particle motions were visualized through an inverted microscope (Nikon

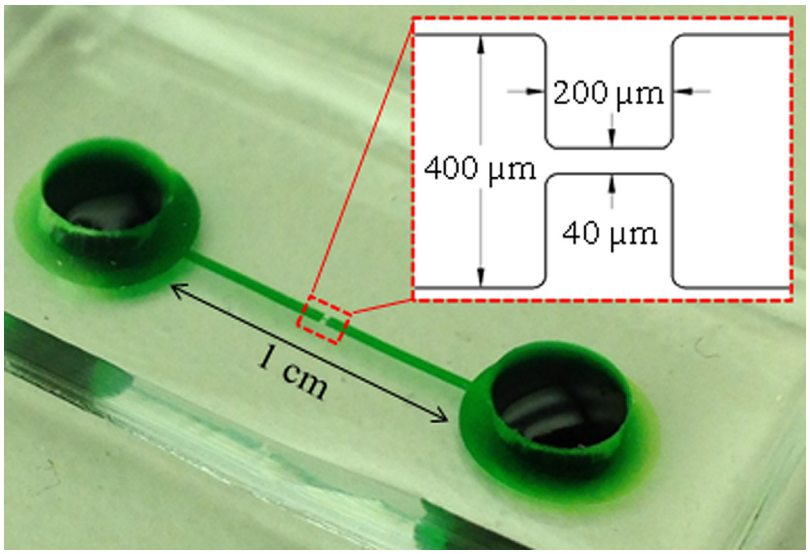

FIG. 1. Picture of the 10:1:10 contraction-expansion microchannel (filled with green food dye for clarity) used in experiments. The inset indicates the dimensions of the constriction.

Eclipse TE2000U, Nikon Instruments) with a CCD camera (Nikon DS-Qi1Mc) at a rate of 15 frames per second. The obtained digital images were post-processed using the Nikon imaging software (NIS-Elements AR 2.30). Particle velocity was determined through dividing the particle travelling distance by the corresponding time interval. The error in reading the pixel number of the particle center was around 1 μm, and the error in the measured particle velocity was estimated to be around 30 μm/s. Particle streak images were obtained by superimposing a sequence of around 150 images.

III. RESULTS AND DISCUSSIONS

A. Comparison of particle electrophoresis in Newtonian and non-Newtonian fluids

Fig. 2 compares the electrophoretic motions of single 10 μm-diameter particles in (a) Newtonian (1 mM buffer) and (b) non-Newtonian (500 ppm PEO in 1 mM buffer) fluids through the microchannel constriction. The average DC electric field across the channel length is 200 V/cm, and particles move from top to bottom in all images for both cases. The suspending fluid also moves from top to bottom in each case, indicating that the channel wall has a higher zeta potential (negative value) than the particle. In the Newtonian fluid, the tracked particle (highlighted by a circle) passes through the constriction quickly as seen from the sequence of images in Fig. 2(a). In contrast, the highlighted single particle in the PEO solution can reach only a half way through the constriction, before it is bounced back toward the entrance of the constriction as demonstrated by the sequential images in Fig. 2(b). Interestingly, this reversing particle overshoots the constriction entrance and then re-enters the constriction to start an oscillation. Moreover, this oscillatory motion seems to be three-dimensional because the particle appears clear and blurred (i.e., in and out of the focal plane) periodically. Since the same amount of Tween 20 was added to both the pure buffer and the PEO solution, we believe the observed difference in particle electrophoresis through the constriction results entirely from the PEO polymer. We have also conducted a quick test of particle electrophoresis in a buffer/glycerol solution and found no oscillating particles in the constriction. Therefore, the increase in solution viscosity alone cannot produce the observed anomalous particle motion.

These distinguished particle electrophoresis behaviors in the two types of suspending fluids can be better identified in Fig. 3, where the transient axial velocities of the two tracked particles in Fig. 2 are compared against time. The time instants greater than 0 s correspond exactly to those labeled on the images of Fig. 2. The time instants smaller than 0 s are included to

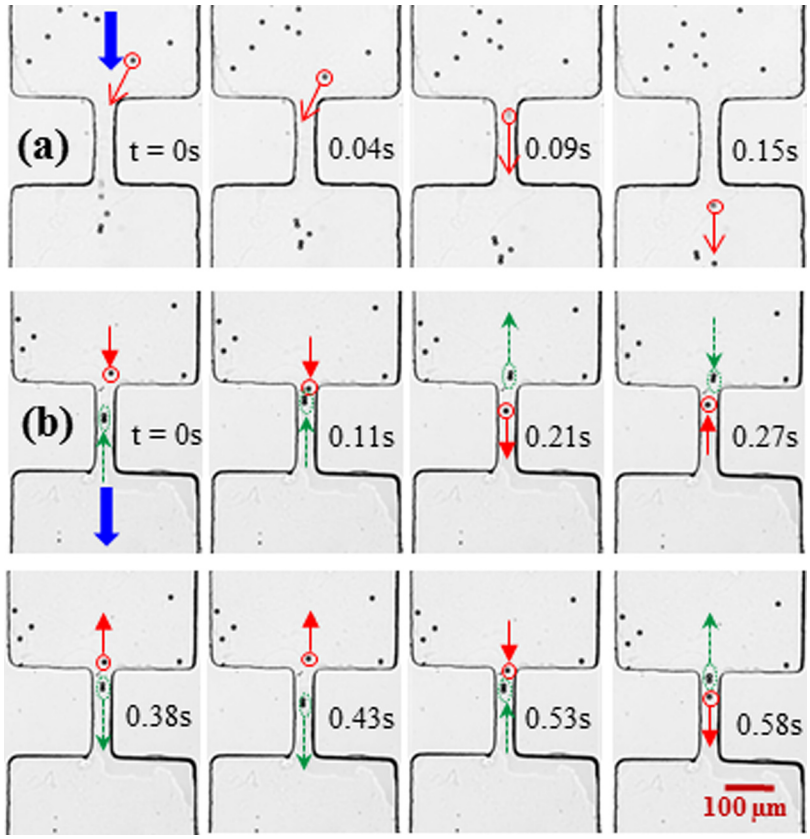

FIG. 2. Sequential images demonstrating the difference of 10 μm particle electrophoresis in (a) Newtonian (1 mM buffer) and (b) non-Newtonian (500 ppm PEO in 1 mM buffer) fluids through the microchannel constriction under an average DC electric field of 200 V/cm. The particles under track are highlighted by a circle (for singles) or an ellipse (for doubles) for a better illustration, where the thin arrows indicate the particle moving directions at the time instants labeled on the images. The block arrows indicate the overall moving directions of the fluids and particles in the channel (Mulitmedia view) [URL: http://dx.doi.org/10.1063/1.4866853.1] [URL: http://dx.doi.org/10.1063/1.4866853.2].

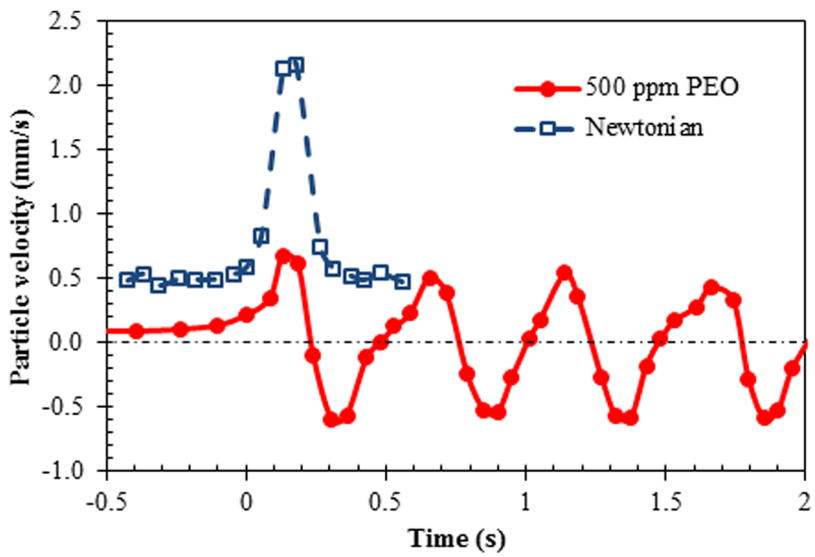

FIG. 3. Comparison of the transient axial velocities of the single particles tracked in the Newtonian and non-Newtonian fluids (see Fig. 2) through the microchannel constriction. Note that the times greater than 0 s correspond to those labeled in Fig. 2 for each fluid. The dashed-dotted line indicates a zero particle velocity.

compare the particle velocities in the two fluids distant from the constriction. The particle in the Newtonian fluid moves at an axial velocity of about 490 μm/s before approaching the constriction, which is more than 5 times larger than that of 85 μm/s for the particle in the non-Newtonian fluid. The Reynolds number based on the particle velocity was thus estimated to be around 0.04 and 3.4×10^{-3} in these two fluids. In the constriction region, the particle in the Newtonian fluid experiences an apparent acceleration followed by a nearly symmetric deceleration, which is consistent with our earlier study.[64] In contrast, the particle in the non-Newtonian fluid undergoes an oscillation with an approximate period of 0.5 s and a maximum speed of about 550 μm/s in both the forward and the backward directions. Using this particle velocity, V_p, we estimated the Weissenberg number ($De = 2\lambda_{eff}V_p/w$ with λ_{eff} and w being the effective relaxation time, see Table I, and constriction width, respectively) or equivalently the Deborah number inside the constriction to be around 0.5.

Single particles in the PEO solution oscillate in the microchannel constriction and are unable to pass through. They can easily get attached to each other forming a particle chain; for example, Fig. 2(b) shows an oscillating two-particle chain (highlighted by a dashed ellipse) in the constriction. The particle chain still oscillates inside the constriction until its length (i.e., the number of particles in the chain) exceeds a certain threshold value. This threshold appears to be a function of electric field and particle size, etc., which will be revisited in the parametric study below (see Sec. III C). The oscillating patterns of particle chains with various lengths are demonstrated in Fig. 4 in the form of their center position vs. time. The oscillating amplitude increases with the number of particles in the chain, and so longer chains tend to move through the constriction with a larger probability. We observed that 10 μm particles can escape from the constriction when a chain of more than 3 particles is formed in 500 ppm PEO solution under the 200 V/cm DC electric field. In addition, the oscillating frequency is found to decrease when the length of the particle chain increases.

B. Attempted explanation of the observed particle oscillation in the non-Newtonian fluid

Anomalous particle motion has been reported in particle sedimentation or rise (e.g., drops and bubbles that are lighter than the fluid) through still viscoelastic fluids,[65–68] which is attributed to either the evolution of a negative wake downstream of the particle,[69–73] or the formation

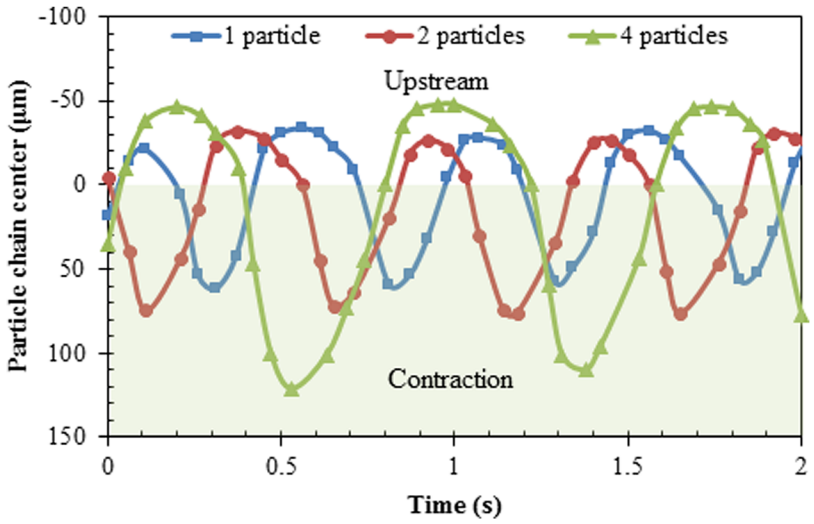

FIG. 4. Tracked center position vs. time for oscillating 10 μm particle chains with various lengths (i.e., the number of particles in the chain) in 500 ppm PEO solution through the microchannel constriction. The average DC electric field is 200 V/cm across the channel length. The shaded zone represents the span of the constriction from 0 to 200 μm.

and breakup of flow-induced structures due to the stress-induced instability.[74–78] The precise mechanism for the particle oscillating phenomenon observed in the PEO solution through the microchannel constriction is currently unknown and deserves intensive future investigations. We speculate that it may be explained using the competition of two forces present in the constriction region as schematically shown in Fig. 5. One is the driving force for the observed electrokinetic particle motion in the microchannel, $\mathbf{F}_{EK}$, which is a combination of fluid electroosmosis, particle electrophoresis and dielectrophoresis, and varies with position in the constriction region.[64] Note that the dielectrophoretic component becomes negligible inside the constriction due to the locally uniform electric field[64]). The other force occurs in the constriction region due to fluid viscoelastic effects (e.g., the flow-induced structures[76–78]), $\mathbf{F}_{VE}$, which resists the fluid shape change (both fluid squeezing and stretching) and hence acts to impede the electrokinetic particle motion. In the Newtonian fluid, $\mathbf{F}_{VE} = 0$ and so $\mathbf{F}_{EK}$ dominates the particle motion, leading to acceleration and deceleration at the entrance and exit of the constriction. In the non-Newtonian fluid, $\mathbf{F}_{VE}$ increases due to the stretch of PEO polymers around the particle when the particle moves along the constriction. Once $\mathbf{F}_{VE}$ exceeds $\mathbf{F}_{EK}$, the particle motion is reversed and the particle is bounced back towards the constriction entrance. With $\mathbf{F}_{VE}$ being decreased during the particle's reverse, $\mathbf{F}_{EK}$ will regain the control of the particle motion and drives the particle into the constriction again. This oscillatory motion continues till a sufficiently long chain of particles is formed, for which $\mathbf{F}_{VE}$ is unable to overcome $\mathbf{F}_{VE}$ in the constriction. As both forces depend on the applied electric field, particle size, and PEO concentration (affect both the rheology of the fluid and the wall/particle zeta potentials[79]), we will investigate their effects on particle oscillation in the following section.

C. Parametric study of particle oscillation in non-Newtonian fluids

1. Electric field effect

Fig. 6(a) shows the snapshot (top) and superimposed (bottom) images of 10 μm particle electrophoresis in 500 ppm PEO solution through the microchannel constriction under the DC electric fields of 100 V/cm (left column), 200 V/cm (middle column), and 400 V/cm (right column), respectively. Particles are uniformly distributed at the upstream of the constriction with a velocity being roughly proportional to the electric field magnitude, which indicates from another angle a shear-rate independent viscosity of the PEO solution. Particles oscillate in the constriction under all electric fields. The oscillating frequency of single particles increases with

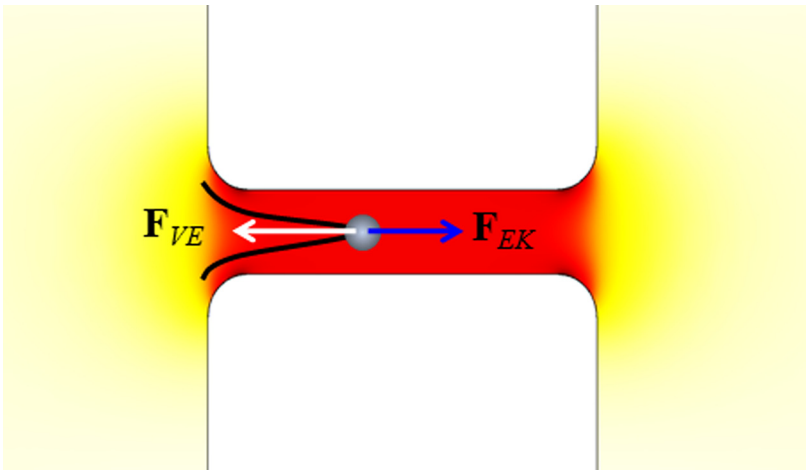

FIG. 5. Schematic illustration of the speculated mechanism for particle oscillation in electrophoresis through a microchannel constriction with a viscoelastic fluid. The background color indicates the electric field contour (the darker the larger magnitude).

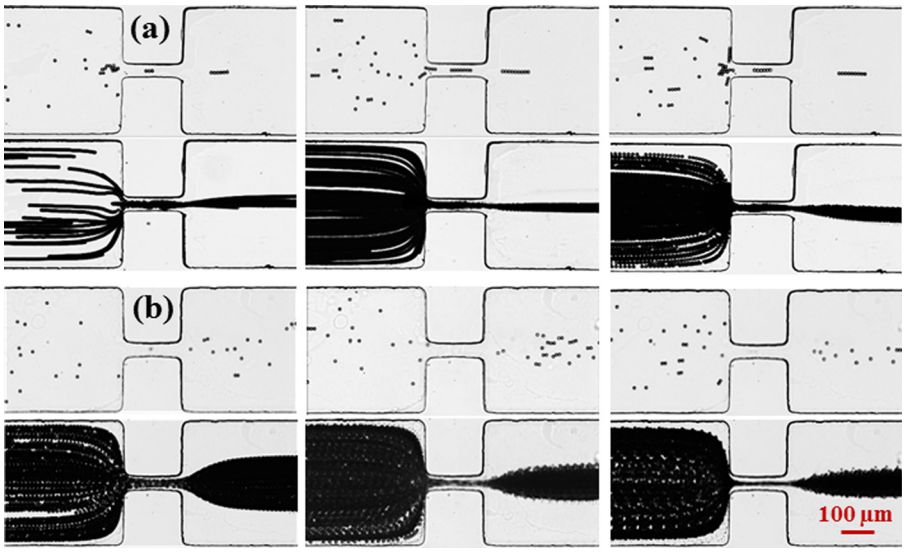

FIG. 6. Snapshot (top) and superimposed (bottom) images illustrating the effects of DC field magnitude on 10 μm particle electrophoresis in (a) non-Newtonian (500 ppm PEO in 1 mM buffer) and (b) Newtonian (1 mM buffer) fluids through the microchannel constriction: 100 V/cm (left column), 200 V/cm (middle column), and 400 V/cm (right column). The fluid flow and particle moving directions are from left to right in all images.

electric field while the oscillating amplitude goes to the opposite. This implies that the viscoelastic effect grows more quickly than the electrokinetic effect (see Fig. 5). As a result, the length threshold of particle chain for passing through the constriction increases at a higher electric field. For example, single particles may escape from the constriction after a few periods of oscillation at 100 V/cm. In contrast, a chain of more than five particles must be formed at 400 V/cm in order for them to travel to the downstream of the constriction. For comparison, Fig. 6(b) shows the images of 10 μm particle electrophoresis in the Newtonian fluid through the constriction, which exhibit an enhanced particle focusing performance with the increase of electric field due to the induced negative dielectrophoresis in the constriction region.[64]

2. PEO concentration effect

Fig. 7 shows the effects of PEO concentration on the oscillation of single 10 μm particles in the microchannel constriction under a 100 V/cm DC field. The variation of particle position before time 0 (at which the tracked particle enters into the constriction) indicates that particle velocity decreases with the increase of PEO concentration. In 50 ppm PEO solution, the particle exhibits a similar behavior to that in the Newtonian fluid, and passes through the constriction without any complication. When the PEO concentration increases to 100 ppm, weak oscillatory motions are observed where some particles pass in a short chain while others can do so in singles after few oscillations in the constriction. For example, the tracked single particle in 100 ppm PEO solution in Fig. 7 escaped from the constriction after one oscillation only. With the further increase of PEO concentration to 200 ppm and 500 ppm, particle oscillations become robust and stable with an increased frequency while a reduced amplitude as seen from Fig. 7. Moreover, longer chains must be formed in order for the particles to move through the constriction. These observations are apparently a consequence of the enhanced viscoelastic effects with the increasing PEO concentration.

3. Particle size effect

Fig. 8 compares the oscillation of single particles of 3 μm, 5 μm, and 10 μm in diameter in 200 ppm PEO solution in the microchannel constriction under a DC electric field of 200 V/cm.

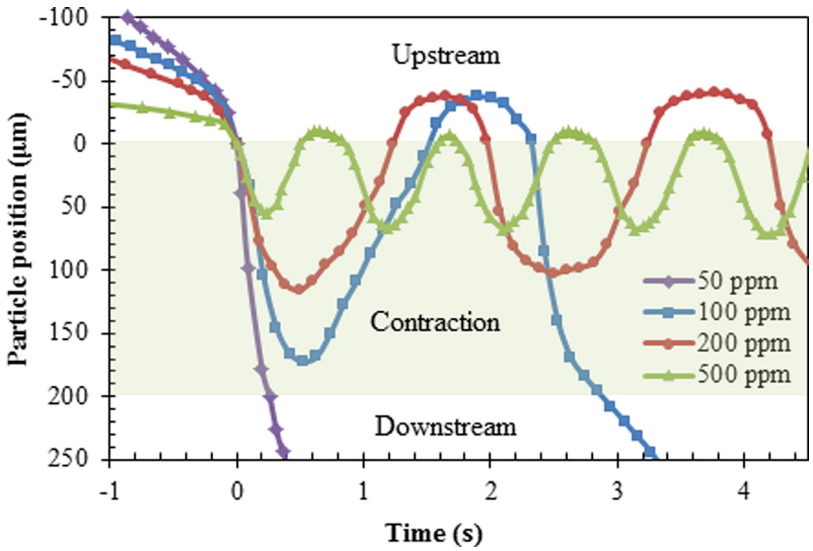

FIG. 7. Effects of PEO concentration (50, 100, 200, and 500 ppm) on the oscillation of single 10 μm particles in the microchannel constriction under 100 V/cm DC electric field. The shaded zone represents the span of the constriction from 0 to 200 μm.

These particles move at a similar velocity before the constriction as seen from the nearly overlapping profiles of particle position vs. time in the range of −0.5 s to 0 s. They all undertake oscillations in the constriction. However, larger particles oscillate faster (i.e., with a higher oscillating frequency) with a smaller amplitude. Moreover, analogous to the effects of electric field (see Fig. 6) and PEO concentration (see Fig. 7) that we presented above, larger particles need to form a longer chain in order to pass through the constriction under the same electric field. Therefore, the viscoelastic force (see Fig. 5) increases with particle size because larger particles cause greater distortions to the suspending viscoelastic fluid than smaller ones do. This also implies that particles with a size smaller than a threshold value may not exhibit the oscillating phenomenon any more, which will be studied in our future work.

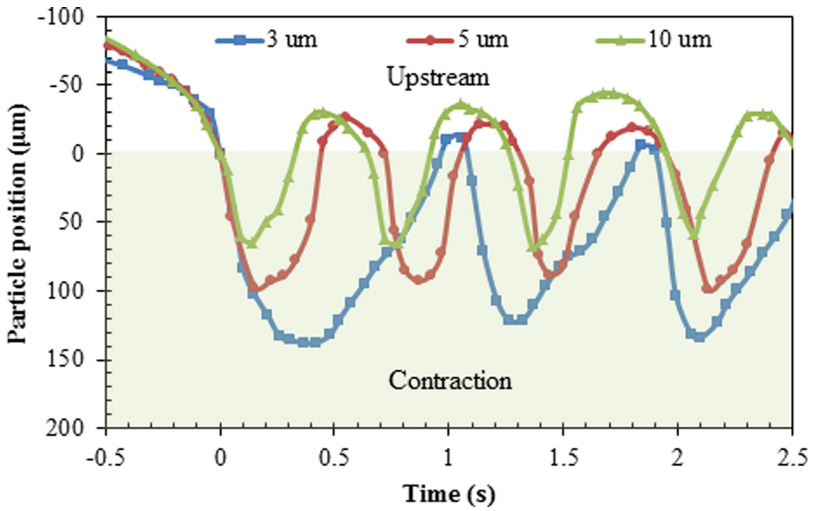

FIG. 8. Effects of particle size (3, 5, and 10 μm in diameter) on the oscillation of single particles in 200 ppm PEO solution in the microchannel constriction under a 200 V/cm DC electric field. The shaded zone represents the span of the constriction from 0 to 200 μm.

IV. CONCLUSIONS

We have conducted an experimental study of the DC electrophoretic motion of particles in viscoelastic PEO solutions through a microchannel constriction. In distinct contrast with the particle electrophoresis in a polymer-free Newtonian fluid, particles in a dilute PEO solution are found to bounce backward halfway in the constriction and bounced again towards downstream at the constriction entrance. Such a stream-wise oscillatory particle motion continues and remains inside the constriction until a sufficient number of particles are attached to form a chain for them to escape. The exact mechanism behind this oscillating phenomenon is currently unclear to us, which is speculated to arise from the competition of a viscoelastic force that is induced in the constriction due to, for example, the flow-induced structures[76–78] and an electrokinetic force. We have also examined the effects of the electric field magnitude, particle size and PEO concentration on the particle oscillation. The increase of either of these parameters can make it more difficult for particles to pass through the constriction. Our future work will find out how the geometry of the constriction may affect the particle electrophoresis in non-Newtonian fluids.

ACKNOWLEDGMENTS

This work was supported in part by NSF under Grant Nos. CBET-0853873 (Xuan) and DMS-1319078 (Qian) and by National Research Foundation of Korea under Grant No. 2011-0014246 (Joo).

[1]D. Li, *Electrokinetics in Microfluidics* (Elsevier Academic Press, Burlington, MA, 2004).
[2]H. C. Chang and L. Y. Yeo, *Electrokinetically Driven Microfluidics and Nanofluidics* (Cambridge University Press, New York, 2010).
[3]S. Qian and Y. Ai, *Electrokinetic Particle Transport in Micro/Nanofluidics: Direct Numerical Simulation Analysis* (CRC Press, 2012).
[4]B. J. Kirby, *Micro- and Nanoscale Fluid Mechanics: Transport in Microfluidic Devices* (Cambridge University Press, 2010).
[5]A. Groisman, M. Enzelberger, and S. Quake, Science **300**, 955–958 (2003).
[6]Y. C. Lam, H. Y. Gan, N. T. Nguyen, and H. Lie, Biomicrofluidics **3**, 014106 (2009).
[7]K. E. Jensen, P. Szabo, F. Okkels, and M. A. Alves, Biomicrofluidics **6**, 044112 (2012).
[8]D. L. Lee, H. Brenner, J. R. Youn, and Y. S. Song, Sci. Rep. **3**, 3258 (2013).
[9]O. L. Hemmingera, P. E. Boukany, S. Q. Wang, and L. J. Lee, J. Non-Newton. Fluid Mech. **165**, 1613–1624 (2010).
[10]P. C. Sousa, F. T. Pinho, M. S. N. Oliveira, and M. A. Alves, Biomicrofluidics **5**, 014108 (2011).
[11]K. Kang, S. S. Lee, K. Hyun, S. J. Lee, and J. M. Kim, Nat. Commun. **4**, 2567 (2013).
[12]Y. J. Kang and S. J. Lee, Biomicrofluidics **7**, 054122 (2013).
[13]R. B. Bird, R. C. Armstrong, and O. Hassager, *Dynamics of Polymeric Liquids* (Wiley-Interscience, 1977), Vol. 1.
[14]C. J. Pipe and G. H. McKinley, Mech. Research Commun. **36**, 110–120 (2009).
[15]X. Hu, P. E. Boukany, O. L. Hemminger, and L. J. Lee, Macromol. Mater. Eng. **296**, 308–320 (2011).
[16]A. Karimi, S. Yazdi, and A. M. Ardekani, Biomicrofluidics **7**, 021501 (2013).
[17]M. S. N. Oliveira, M. A. Alves, and F. T. Pinho, *Transport and Mixing in Laminar Flows: From Microfluidics to Oceanic Currents*, 1st ed., edited by R. Grigoriev (Wiley-VCH, 2012).
[18]C. L. A. Berli, Electrophoresis **34**, 622–630 (2013).
[19]C. Zhao and C. Yang, Adv. Colloid. Interface Sci. **201–202**, 94–108 (2013).
[20]S. Das and S. Chakraborty, Anal. Chim. Acta **559**, 15–24 (2006).
[21]S. Chakraborty, Anal. Chim. Acta **605**, 175–184 (2007).
[22]C. L. A. Berli and M. L. Olivares, J. Colloid Interface Sci. **320**, 582–589 (2008).
[23]C. Zhao, E. Zholkovskij, J. H. Masliyah, and C. Yang, J. Colloid Interface Sci. **326**, 503–510 (2008).
[24]G. H. Tang, X. F. Li, Y. L. He, and W. Q. Tao, J. Non–Newtonian Fluid Mech. **157**, 133–137 (2009).
[25]M. L. Olivares, L. Vera-Candioti, and C. L. A. Berli, Electrophoresis **30**, 921–929 (2009).
[26]C. Zhao and C. Yang, Electrophoresis **31**, 973–979 (2010).
[27]M. Hadigol, R. Nosrati, and M. Raisee, Colloid Surf. A **374**, 142–153 (2011).
[28]A. Babaie, A. Sadeghi, and M. H. Saidi, J. Non-Newtonian Fluid Mech. **185–186**, 49–57 (2012).
[29]Y. J. Chang, P. W. Yang, and H. F. Huang, J. Non-Newtonian Fluid Mech. **194**, 32–41 (2013).
[30]C. Zhao and C. Yang, Electrophoresis **34**, 662–667 (2013).
[31]A. M. Afonso, M. A. Alves, and F. T. Pinho, J. Non-Newtonian Fluid Mech. **159**, 50–63 (2009).
[32]S. Dhinakaran, A. M. Afonso, M. A. Alves, and F. T. Pinho, J. Colloid Interf. Sci. **344**, 513–520 (2010).
[33]J. J. Sousa, A. M. Afonso, F. T. Pinho, and M. A. Alves, Microfluid. Nanofluid. **10**, 107–122 (2011).
[34]A. M. Afonso, F. T. Pinho, and M. A. Alves, J. Non-Newtonian Fluid Mech. **179–180**, 55–68 (2012).
[35]W. Choi, S. Woo Joo, and G. Lim, J. Non-Newtonian Fluid Mech. **187–188**, 1–7 (2012).
[36]A. M. Afonso, M. A. Alves, and F. T. Pinho, J. Colloid Interface Sci. **395**, 277–286 (2013).
[37]W. B. Zimmerman, J. M. Rees, and T. J. Craven, Microfluid. Nanofluid. **2**, 481–492 (2006).
[38]T. J. Craven, J. M. Rees, and W. B. Zimmerman, Microfluid. Nanofluid. **9**, 559–571 (2010).

[39]C. Zhao and C. Yang, Biomicrofluidics **5**, 014110 (2011).
[40]C. Zhao and C. Yang, Appl. Math. Comput. **211**, 502–509 (2009).
[41]H. M. Park and W. M. Lee, J. Colloid Interface Sci. **317**, 631–636 (2008).
[42]Q. Liu, Y. Jian, and L. Yang, J. Non-Newtonian Fluid Mech. **166**, 478–486 (2011).
[43]C. O. Ng, J. Non-Newtonian Fluid Mech. **198**, 1–9 (2013).
[44]E. Lee, Y. F. Huang, and J. P. Hsu, J. Colloid Interface Sci. **258**, 283–288 (2003).
[45]E. Lee, C. S. Tsai, J. Hsu, and C. J. Chen, Langmuir **20**, 7952–7959 (2004).
[46]E. Lee, C. T. Chen, and J. P. Hsu, J. Colloid Interface Sci. **285**, 857–864 (2005).
[47]J. P. Hsu, L. H. Yeh, and M. H. Ku, Colloid Polym. Sci. **284**, 886–892 (2006).
[48]J. P. Hsu and L. H. Yeh, Langmuir **23**, 8637–8646 (2007).
[49]J. P. Hsu, L. H. Yeh, and S. J. Yeh, J. Phys. Chem. B **111**, 12351–12631 (2007).
[50]L. H. Yeh and J. P. Hsu, Microfluid. Nanofluid. **7**, 383–392 (2009).
[51]J. P. Hsu, C. Y. Chen, L. H. Yeh, and S. Tseng, Colloid Surface B **69**, 8–14 (2009).
[52]A. S. Khair, D. E. Posluszny, and L. M. Walker, Phys. Rev. E **85**, 016320 (2012).
[53]F. A. Morrison, J. Colloid Interface Sci. **34**, 210–214 (1970).
[54]F. M. Chang and H. K. Tsao, Appl. Phys Lett. **90**, 194105 (2007).
[55]R. M. Bryce and M. R. Freeman, Phys. Rev. E **81**, 036328 (2010).
[56]R. M. Bryce and M. R. Freeman, Lab Chip **10**, 1436–1441 (2010).
[57]W. W. Graessley, Polymer **21**, 258–262 (1980).
[58]D. F. James, Annu. Rev. Fluid Mech. **41**, 129–142 (2009).
[59]L. E. Rodd, J. J. Cooper-White, D. V. Boger, and G. H. McKinley, J. Non-Newtonian Fluid Mech. **143**, 170–191 (2007).
[60]M. Rubinstein and R. H. Colby, *Polymer Physics* (Oxford University Press Inc., 2003).
[61]V. Tirtaatmadja, G. H. Mckinley, and J. J. Cooper-White, Phys. Fluid **18**, 043101 (2006).
[62]J. Zhu, S. Sridharan, G. Hu, and X. Xuan, J. Micromech. Microeng. **22**, 075011 (2012).
[63]A. Kale, S. Patel, G. Hu, and X. Xuan, Electrophoresis **34**, 674–683 (2013).
[64]J. Zhu and X. Xuan, Electrophoresis **30**, 2668–2675 (2009).
[65]G. H. McKinley, *Transport Processes in Bubbles, Drops & Particles*, 2nd ed., edited by R. Chhabra, D. De Kee (Taylor & Francis, 2001), Chap. 14.
[66]L. E. Becker, G. H. McKinley, H. K. Rasmussen, and O. Hassager, J. Rheol. **38**, 377–403 (1994).
[67]C. Bodart and M. J. Crochet, J. Non-Newton. Fluid Mech. **54**, 303–329 (1994).
[68]W. M. Jones, A. H. Price, and K. Walters, J. Non-Newton. Fluid Mech. **53**, 175–196 (1994).
[69]M. J. King and N. D. Waters, J. Phys. D **5**, 141–150 (1972).
[70]R. Zheng and N. Phan-Thien, Rheol. Acta **31**, 323–332 (1992).
[71]M. B. Bush, J. Non-Newtonian Fluid Mech. **55**, 229–247 (1994).
[72]M. T. Arigo and G. H. Mckinley, J. Rheol. **41**, 103–128 (1997).
[73]M. T. Arigo and G. H. Mckinley, Rheol. Acta **37**, 307–327 (1998).
[74]S. Chen and J. P. Rothstein, J. Non-Newtonian Fluid Mech. **116**, 205–234 (2004).
[75]S. von Kann, J. H. Snoeijer, and D. van der Meer, Phys. Rev. E **87**, 042301 (2013).
[76]A. M. Mollinger, E. C. Cornelissen, and B. H. A. A. van den Brule, J. Non-Newtonian Fluid Mech. **86**, 389–393 (1999).
[77]N. Kumar, S. Majumdar, A. Sood, R. Govindarajan, S. Ramaswamy, and A. K. Sood, Soft Matter **8**, 4310–4313 (2012).
[78]A. Jayaraman and A. Belmonte, Phys. Rev. E **67**, 065301(R) (2003).
[79]J. Horvath and V. Dolnik, Electrophoresis **22**, 644–655 (2001).
[80]L. E. Rodd, T. P. Scott, D. V. Boger, J. J. Cooper-White, and G. H. McKinley, J. Non–Newtonian Fluid Mech. **129**, 1–22 (2005).